IEEE Access
Multidisciplinary ⋮ Rapid Review ⋮ Open Access Journal

Received August 12, 2021, accepted August 27, 2021, date of publication September 3, 2021, date of current version September 15, 2021.

Digital Object Identifier 10.1109/ACCESS.2021.3109938

Antenna Array Thinning Through Quantum Fourier Transform

PAOLO ROCCA[1,2], (Senior Member, IEEE), NICOLA ANSELMI[1], (Member, IEEE), GIACOMO OLIVERI[1], (Senior Member, IEEE), ALESSANDRO POLO[1], (Member, IEEE), AND ANDREA MASSA[1,3,4], (Fellow, IEEE)

[1]CNIT–"University of Trento" Research Unit, 38123 Trento, Italy
[2]ELEDIA Research Center (ELEDIA@XIDIAN—Xidian University), Xi'an, Shaanxi 710071, China
[3]ELEDIA Research Center (ELEDIA@UESTC—UESTC), School of Electronic Engineering, Chengdu 611731, China
[4]ELEDIA Research Center (ELEDIA@TSINGHUA—Tsinghua University), Haidian, Beijing 100084, China

Corresponding author: Andrea Massa (andrea.massa@unitn.it)

This work benefited from the networking activities carried out within the Project Cloaking Metasurfaces for a New Generation of Intelligent Antenna Systems (MANTLES) (Grant No. 2017BHFZKH) funded by Italian Ministry of Education, University, and Research under the PRIN2017 Program (CUP: E64I19000560001). Moreover, it benefited from the networking activities carried out within the Project SPEED (Grant No. 61721001) funded by the National Science Foundation of China under Chang-Jiang Visiting Professorship Program, the Project "Inversion Design Method of Structural Factors of Conformal Load-bearing Antenna Structure based on Desired EM Performance Interval" (Grant no. 2017HZJXSZ) funded by the National Natural Science Foundation of China, and the Project "Research on Uncertainty Factors and Propagation Mechanism of Conformal Loab-bearing Antenna Structure" (Grant No. 2021JZD-003) funded by the Department of Science and Technology of Shaanxi Province within the Program Natural Science Basic Research Plan in Shaanxi Province.

ABSTRACT Thinning antenna arrays through quantum Fourier transform (*QFT*) is proposed. Given the lattice of the candidate locations for the array elements, the problem of selecting which antenna location has to be either occupied or not by an array element is formulated in the quantum computing (*QC*) framework and then addressed with an *ad-hoc* design method based on a suitable implementation of the *QFT* algorithm. Representative numerical results are presented and discussed to point out the features and the advantages of the proposed *QC*-based thinning technique.

INDEX TERMS Antenna array synthesis, quantum computing, quantum Fourier transform, thinned antenna array.

I. INTRODUCTION

Phased array (*PA*) is a more and more popular antenna technology [1], [2] for a wide range of modern applications such as 5G communications [3]– [5], anti-collision and navigation systems for autonomous driving and unmanned vehicles [6]– [8], future weather and air traffic control radars [9]– [11], and biomedical imaging and therapy [12], [13]. However, minimizing the complexity and the costs of *PA*s is still an open issue of great scientific and industrial interest to enable the diffuse use of *PA*s in a huge number of commercial systems and applications. Towards this end, several studies have been carried out to develop unconventional architectures for cost-effective and high-performance *PA* solutions [14]. Indeed, classical *PA*s consist of bulky and expensive [15] fully-populated arrangements where each antenna element has a dedicated transmit-receive module (*TRM*), composed by an amplifier and a phase shifter for the signal transmission and reception, as well as a radio-frequency (*RF*) chain. Differently, unconventional *PA*s need a reduced number of *TRM*s and *RF* chains since they consider either clustered [16]– [20], or sparse [21]– [24], or thinned [25]– [33] layouts. As for these latter, the radiation pattern is controlled by turning off or removing a set of the elements from an initial fully-populated regular lattice to yield a spatial tapering [1] on the array aperture and, for instance, low sidelobes [2]. The antenna elements are usually uniformly fed so that the *TRM* amplifiers are all saturated to achieve the maximum efficiency and to avoid output power wastening. In this case, only the phase shifters are used for scanning the main beam along the desired direction. Otherwise, alternative thinned architectures exploit tunable amplifiers for controlling the beam shape [34], [35], while off-elements are connected to matched loads instead of being removed. This allows one to maintain a regular distribution of the elements, thus more uniform and predictable electromagnetic coupling conditions.

The associate editor coordinating the review of this manuscript and approving it for publication was Abdullah Iliyasu.

To select which elements to keep, different design techniques have been proposed. In [25], the thinning of large arrays has been carried out with a random process to match a desired spatial taper, while the arising statistical radiation performance (i.e., sidelobe level, beamwidth, and directivity) have been then studied in [26]. Recently, thanks to the growth of the computational capabilities and the engineering use of advanced stochastic (i.e., global) optimization techniques, thinning methods based on the Simulated Annealing [27], Genetic Algorithms [28], [29], Particle Swarm Optimization [30], and Ant Colony Optimization [31] have been introduced by formulating the synthesis problem as the minimization of a cost function that quantifies the mismatch between the desired radiation performance and the ones iteratively-synthesized. Although global optimization methods theoretically avoid local minima (i.e., sub-optimal solutions) due to the non-convexity of the cost function at hand, their computational cost is usually very high. Dealing with massively thinned arrays [32], analytic methodologies based on Difference Sets (*DS*) and Almost Difference Sets (*ADS*) (i.e., analytic binary sequences that define which elements of the array lattice have to be either off or on) have been also studied since the discrete values of the Fourier transform of the autocorrelation of these binary sequences coincide with samples of the radiation pattern. Such a property has been then exploited to synthesize thinned arrays fitting user-constrained autocorrelation functions instead of power pattern masks [33]. Unfortunately, *DS* and *ADS* sequences are available only for a limited set of array apertures, geometries, and thinning factors.[1]

This paper presents a novel method for *PA* thinning based on quantum computing (*QC*). Nowadays, *QC* is gaining a growing attention since it proved to be able to drastically speed-up the solution of complex problems when properly formulated within the quantum mechanics framework, which is at the basis of *QC* [36]. Today, the main limitation of *QC* is the realization of quantum computers working with a large number of quantum bits (called *qubits*). Nevertheless, quantum algorithms and approaches have been developed to address, even with classical supercomputers, computationally-hard problems in a reasonable amount of time. More specifically, the quantum Fourier transform (*QFT*) [37] is here applied for the first time, to the best of the authors' knowledge, to synthesize thinned antenna arrays. Likewise the discrete Fourier transform (*DFT*), the *QFT* performs a discrete Fourier transform on a list of complex numbers, but the observable (i.e., measurable) outputs are the probabilities of the corresponding quantum states (i.e., real values) [38] instead of the Fourier-transformed coefficients of the input values. However, since the relationship between the coefficients of an array with the elements uniformly-spaced on a rectangular grid and the array factor is a Fourier transform, the idea is to still exploit the *QFT* output to thin the array by keeping the elements of the lattice whose corresponding quantum state probability is greater than a user-defined threshold. Moreover, the probability of the quantum states is used to define the excitations in case of non-uniform arrays with controllable amplifiers to enable an enhanced control of the arising radiation features.

The rest of the paper is organized as follows. In Sect. II, the array thinning problem is mathematically formulated in the *QC* framework by presenting the *QFT*-based synthesis method, as well. Selected numerical results are then (Sect. III) reported to validate the proposed method as well as to analyze and assess its performance in comparison with the classical *DFT* algorithm, as well. Eventually, some conclusions and final remarks are drawn (Sect. IV).

II. MATHEMATICAL FORMULATION

Let us consider a linear antenna array of N elements equally-spaced along the z-axis, d being the inter-element distance. Each n-th ($n = 0, \ldots, N-1$) element is equipped with a *TRM* that provides an amplitude weight and a phase delay equal to α_n and φ_n, respectively. The array radiates the following radiation pattern [1]

$$\mathbf{E}(u) = \sum_{n=0}^{N-1} w_n \mathbf{f}_n(u) \exp[j(kdu)n] \tag{1}$$

where w_n ($w_n \triangleq \alpha_n \exp[j\varphi_n]$) is the n-th ($n = 0, \ldots, N-1$) complex excitation, $k = \frac{2\pi}{\lambda}$ is the free-space wavenumber, λ being the corresponding wavelength, u ($u \triangleq \cos\theta$, $-1 \leq u \leq 1$) is the direction cosine, θ ($0 \leq \theta \leq \pi$) being the angular direction from the array axis, and $j = \sqrt{-1}$. Under the assumption that the radiation pattern of the n-th ($n = 0, \ldots, N-1$) elementary radiator of the array is equal for all the antennas (i.e., $\mathbf{f}_n(u) = \mathbf{f}(u)$; $n = 0, \ldots, N-1$), it turns out that $\mathbf{E}(u) \simeq \mathbf{f}(u)\mathcal{A}(u)$, $\mathcal{A}(u)$ being the array factor function given by

$$\mathcal{A}(u) = \sum_{n=0}^{N-1} w_n \exp[j(kdu)n]. \tag{2}$$

The thinning of the array is mathematically modeled by introducing a Boolean vector, $\mathbf{B} = \{b_n;\ n = 0, \ldots, N-1\}$, where $b_n \in \{0,\ 1\}$ is a binary entry used to indicate whether to keep the n-th array element in the array or to turn-off/remove it. More specifically, if $b_n = 1$ then the n-th ($n = 0, \ldots, N-1$) *TRM* is connected to the beam-forming network (*BFN*) and the amplitude coefficient is either uniform (i.e., $w_n = 1.0$) or continuous (i.e., $w_n \in \mathbb{R}_{>0}$, $\mathbb{R}_{>0}$ being the set of positive real numbers greater than zero) for isophoric or non-uniform thinned array, respectively. Otherwise (i.e., $b_n = 0$), the n-th ($n = 0, \ldots, N-1$) array element has no *TRM* and it is terminated on a matched load (i.e., it does not contribute to the signal transmission and reception through the *BFN*). According to this description, $w_n \rightarrow w_n b_n$ ($n = 0, \ldots, N-1$) in (2) and the degrees of freedom (*DoF*s) of the thinning problem are the binary entries of the Boolean vector $\mathbf{B}$. The synthesis problem at hand can be then stated as follows:

[1]The thinning factor is defined as the percentage of active/on elements with respect to all the possible candidate element positions in the lattice.

Antenna Array Thinning Problem (*AATP*) - Given a uniform lattice of N candidate locations equally-space by d, determine the N entries of the Boolean vector $\mathbf{B}$ to minimize the cost function $\Psi(\mathbf{B})$ defined as the square distance between a 'feature' of the reference pattern, $\mathbb{G}\left\{\mathcal{A}^{ref}(u)\right\}$, and that of the thinned one, $\mathbb{G}\{\mathcal{A}(u\,|\,\mathbf{B})\}$

$$\Psi(\mathbf{B}) = \int_{-1}^{1} \left| \mathbb{G}\{\mathcal{A}(u\,|\,\mathbf{B})\} - \mathbb{G}\left\{\mathcal{A}^{ref}(u)\right\} \right|^2 du. \quad (3)$$

In order to solve the *AATP*, a design strategy based on the *QFT* is presented hereinafter starting from the following observations:

- the relationship between the samples of the array pattern function and the array excitations is a *DFT*;
- the *DFT* of the array excitations provides the least mean squared error approximation of the desired pattern when $d \geq \frac{\lambda}{2}$ [1], [2], thus guarantees the minimum value of (3) when $\mathbb{G}\left\{\mathcal{A}^{ref}(u)\right\}$ is set as the array factor function, namely $\mathbb{G}\left\{\mathcal{A}^{ref}(u)\right\} = \mathcal{A}^{ref}(u)$;
- the *QFT* algorithm is the natural extension to the quantum regime of the *DFT* with a computational complexity of order $\mathcal{O}\left((\log N)^2\right)$ instead of $\mathcal{O}(N \times \log N)$ of the classical *DFT*. It means that the exploitation of the quantum superposition and parallelism can provide an exponential speed-up with respect to standard implementations;
- unlike the *DFT*, the *QFT* gives the probability (i.e., real positive numbers) of the Fourier-transformed input set instead of the complex Fourier values.

Accordingly, the following method has been derived. From (2), it turns out that the sequence/discrete-dataset of N complex samples of the array factor, $\mathbf{A}$ ($\mathbf{A} = \{\mathcal{A}_m;\ m = 0, \ldots, N-1\}$), is the *DFT* of the sequence/discrete-dataset of the N complex excitations, $\mathbf{w}$ ($\mathbf{w} = \{w_n; n = 0, \ldots, N-1\}$),

$$\mathbf{A} = DFT\{\mathbf{w}\} \quad (4)$$

so that the m-th ($m = 0, \ldots, N-1$) entry of $\mathbf{A}$, $\mathcal{A}_m$, ($\mathcal{A}_m \triangleq \mathcal{A}(u_m)$, u_m being the m-th sample along the angular cosine direction given by $u_m = -m\frac{\lambda}{N \times d}$ [1]) is equal to [1]

$$\mathcal{A}_m = \sum_{n=0}^{N-1} w_n \exp\left[-j\left(\frac{2\pi}{N}n\right)m\right]. \quad (5)$$

Once the pattern samples are defined, $\mathbf{A}$, the array factor function (2) is yielded as the summation of weighted periodic sinc functions

$$\mathcal{A}(u) = \sum_{m=0}^{N-1} \mathcal{A}_m \mathbb{S}\left(\pi du + \frac{m\pi}{N}\right) \quad (6)$$

being $\mathbb{S}(x) \triangleq \frac{\sin(Nx)}{N\sin(x)}$.

Vice-versa, the complex excitation set $\mathbf{w}$ is the inverse discrete Fourier transform (*IDFT*) of the discrete dataset of the pattern samples, $\mathbf{A}$

$$\mathbf{w} = IDFT\{\mathbf{A}\} \quad (7)$$

being $w_n = \frac{1}{N}\sum_{m=0}^{N-1} \mathcal{A}_m \exp\left[j\left(\frac{2\pi}{N}m\right)n\right]$ and the array factor function (2) is obtained by substituting $\mathbf{w}$ in (2).

Moving to the quantum framework, let us define the *input quantum state vector* $|\mathbf{A}\rangle$ starting from the N-size set of complex pattern samples $\mathbf{A}$ and considering L ($L \triangleq \log_2 N$) single-qubits/1-qubits, $\{|s_\ell\rangle;\ \ell = 1, \ldots, L\}$, each having two possible states $|s_\ell\rangle = \{|0\rangle, |1\rangle\}$ (called *kets* in the language of the Dirac notation [38])

$$|\mathbf{A}\rangle = \sum_{m=0}^{N-1} \widehat{\mathcal{A}}_m |\mathbf{a}_m\rangle \quad (8)$$

where $\widehat{\mathcal{A}}_m$ ($\widehat{\mathcal{A}}_m \triangleq \frac{\mathcal{A}_m}{\|\mathbf{A}\|}$, $\|.\|$ being the norm operator) is the complex amplitude of the m-th ($m = 0, \ldots, N-1$) L-qubit, $|\mathbf{a}_m\rangle$, given by $|\mathbf{a}_m\rangle = |s_L\ s_{L-1}, \ldots, s_\ell, \ldots, s_1\rangle$ where $|s_L\ s_{L-1}, \ldots, s_\ell, \ldots, s_1\rangle$ stands for the concatenation of the L single-qubits, $\{|s_\ell\rangle;\ \ell = 1, \ldots, L\}$ ($|s_L s_{L-1} \ldots s_\ell \ldots s_1\rangle \triangleq \bigotimes_{\ell=L}^{1} |s_\ell\rangle$) .[2] Analogously to the classical theory, the *output quantum state vector* $|\mathbf{w}\rangle$

$$|\mathbf{w}\rangle = \sum_{n=0}^{N-1} \widehat{w}_n |\mathbf{a}_n\rangle \quad (9)$$

is the *IQFT* of the *input quantum state vector* $|\mathbf{A}\rangle$ (i.e., $|\mathbf{w}\rangle = IQFT\{|\mathbf{A}\rangle\}$) where $\widehat{w}_n$ ($n = 0, \ldots, N-1$) is a normalized complex value equal to $\widehat{w}_n = \frac{w_n}{\|\mathbf{w}\|}$, w_n being derived by $\mathbf{A}$ as in (7) through *IDFT*.

However, it worth pointing out that there is no way to retrieve/measure/observe the (complex) values of the N entries of $\widehat{\mathbf{w}}$ ($\widehat{\mathbf{w}} = \{\widehat{w}_n; n = 0, \ldots, N-1\}$) at the output of the *IQFT* operation (i.e., from $|\mathbf{w}\rangle$), but only the probability p_n ($n = 0, \ldots, N-1$) that the output quantum state vector $|\mathbf{w}\rangle$ would be equal to the n-th ($n = 0, \ldots, N-1$) L-qubit $|\mathbf{a}_n\rangle$. On the other hand, the following relation between the probability p_n ($n = 0, \ldots, N-1$) and $\widehat{w}_n$ ($n = 0, \ldots, N-1$) holds true [38]

$$p_n = |\widehat{w}_n|^2. \quad (10)$$

On the basis of the above considerations, the following algorithm, performed according to the a multi-step procedure based on the exploitation of the *IQFT* and the measurable quantities at the output of the *QC*, is proposed for array thinning:

- *Step 1* - ***Initialization.*** Given the number of candidate array elements N and the inter-element distance d, define the reference array pattern, $\mathcal{A}^{ref}(u)$, and choose the desired pattern 'feature', $\mathbb{G}\left\{\mathcal{A}^{ref}(u)\right\}$, to be matched in the least-square sense (3) within a user-defined confidence threshold η (i.e., $\Psi(\mathbf{B}) \leq \eta$);
- *Step 2* - ***QFT Application.*** Apply the *IQFT* to the input quantum state vector $|\mathbf{A}\rangle$ (8) and measure the probability p_n ($n = 0, \ldots, N-1$) associated to the output quantum state vector $|\mathbf{w}\rangle$ (9);

[2] In an explicit form: $\bigotimes_{\ell=L}^{1} |s_\ell\rangle \triangleq |s_L\rangle \bigotimes \ldots \bigotimes |s_\ell\rangle \ldots \bigotimes \ldots \bigotimes |s_1\rangle$, $\bigotimes$ being the tensor product.

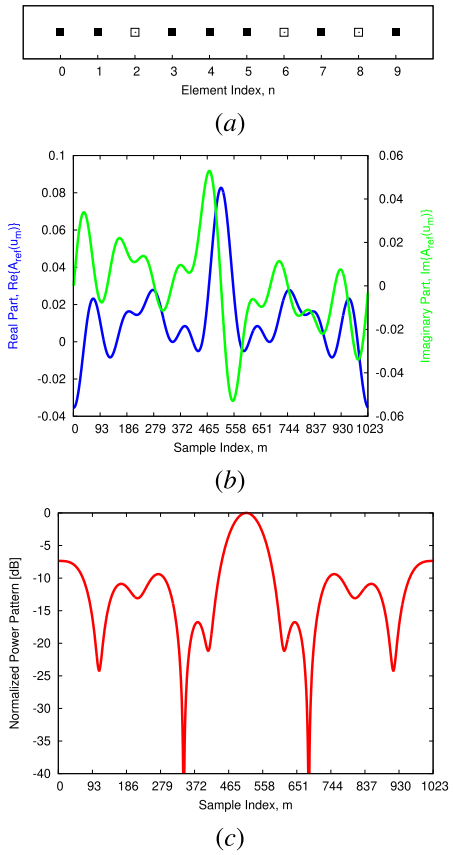

FIGURE 1. ***Numerical Validation*** **- Reference thinned layout (*a*). Plot of the *N* samples of (*b*) the array factor, $\mathbf{A}^{ref} = \{\mathcal{A}_m^{ref};\ m = 0, \ldots, N-1\}$, and of (*c*) the corresponding normalized power pattern, $\mathbf{P}^{ref} = \{\mathcal{P}_m^{ref};\ m = 0, \ldots, N-1\}$ ($\mathcal{P}_m \triangleq |\mathcal{A}_m|^2$).**

- *Step 3* - ***Probability Ranking.*** Order the N observed probabilities (10) of the output quantum state vector from the highest $\hat{p}_t\big\rfloor_{t=0} = \max_n \{p_n\}$ down to the lowest $\hat{p}_t\big\rfloor_{t=N-1} = \min_n \{p_n\}$ ($0 \le t \le N-1$). In case of equal probability values, rank them according to the value of the n-th ($n = 0, \ldots, N-1$) index, namely $\hat{p}_t = p_{n_1}$ and $\hat{p}_{t+1} = p_{n_2}$ if $p_{n_1} = p_{n_2}$ and $n_1 < n_2$ ($n_1,\ n_2 \in [0 : N-1]$);
- *Step 4* - ***Thinned Array Synthesis.*** Keep 'on' the minimum number of first K elements among the N candidates ($K \le N$) of the ordered list defined at *Step 3* whose corresponding thinned array (i.e., Boolean vector $\mathbf{B}^{opt}$) affords a radiation pattern, $\mathcal{A}\left(u \,|\, \mathbf{B}^{opt}\right)$, that satisfies the matching condition

$$\Psi\left(\mathbf{B}^{opt}\right) \le \eta, \tag{11}$$

η being the matching threshold, where the n-th ($n = 0, \ldots, N-1$) entry of the thinning Boolean vector $\mathbf{B}^{opt}$ is set to $b_n = 1$ ($b_n = 0$) if the value of the corresponding t-th probability ($n \leftarrow t$) lies (does not lie) within the range $0 \le t \le K-1$

$$b_n\big\rfloor_{n \leftarrow t} = \begin{cases} 1 \ \textit{if} \ \ 0 \le t \le (K-1) \\ 0 \ \textit{if} \ \ K \le t \le (N-1) \end{cases} \tag{12}$$

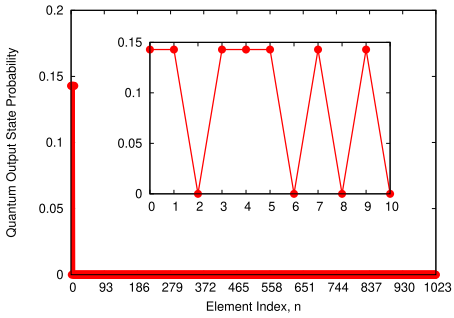

FIGURE 2. ***Numerical Validation*** **- Plot of the probability, p_n ($n = 0, \ldots, N-1$), that the output quantum state vector $|\mathbf{w}\rangle$ is equal to the *n*-th ($n = 0, \ldots, N-1$) *L*-qubit $|\mathbf{a}_n\rangle$.**

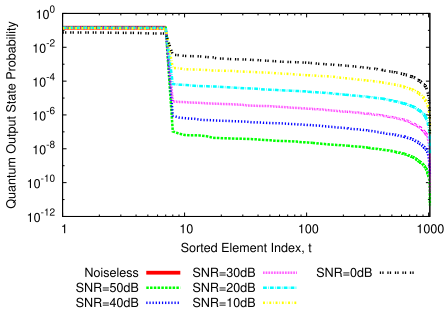

FIGURE 3. ***Numerical Analysis*** **- Plot of the sorted probability value, p_t ($t = 0, \ldots, N-1$), that the output quantum state vector $|\mathbf{w}\rangle$ is equal to the *t*-th ($t = 0, \ldots, N-1$) *L*-qubit $|\mathbf{a}_t\rangle$, when blurring the amplitudes of the input quantum vector, $\widehat{\mathbf{A}}^{ref}$, with a Gaussian additive noise characterized by a signal-to-noise ratio equal to *SNR*.**

Moreover, set the n-th ($n = 0, \ldots, N-1$) amplitude excitation to either $w_n = 1.0$ (uniformly-excited array) or to $w_n = \sqrt{p_n}$ (non-uniformly excited array) if $b_n = 1$, while turn off the n-th ($n = 0, \ldots, N-1$) elements otherwise (i.e., $b_n = 0$).

If there is no thinned solution $\mathbf{B}$ that fits (11), relax the value of η or, if doable having a wider antenna aperture, increase N.

III. NUMERICAL VALIDATION

In this section, the *QFT*-based approach for thinning antenna arrays is firstly validated, then selected numerical results are reported and discussed to analyze the robustness of the *QC*-thinning method against the noise on the input data and to assess its performance also in comparison with the classical *DFT*-based implementation. The quantum numerical simulations have been carried out within the Qiskit open source framework [39] by using the IBM Quantum cloud platform [40]. In all simulations, ideal radiating elements (i.e., $\mathbf{f}(u) = 1$) have been considered to focus the attention on the array factor, which is the function optimized by the proposed synthesis method.

In the first example (*Validation*), the linear thinned array has been assumed to be known. It has been generated by thinning an isophoric ($w_n = 1; n = 0, \ldots, N-1$) fully-populated

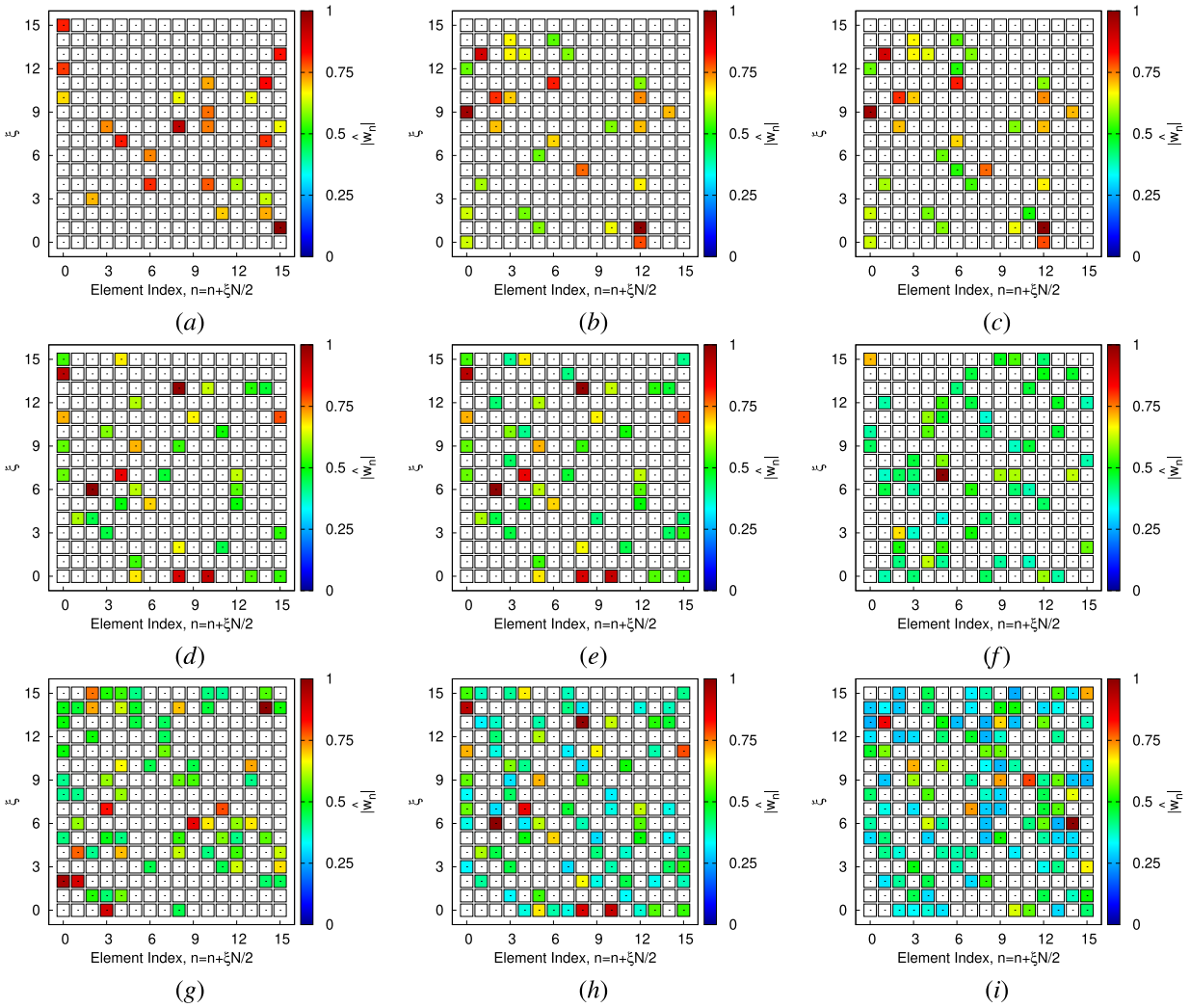

FIGURE 4. ***Numerical Assessment*** **- *QC*-synthesized thinned layouts when (*a*)(*b*)(c) $SLL_{ref} = -10$ [dB], (*d*)(*e*)(*f*) $SLL_{ref} = -12.5$ [dB], and (*g*)(*h*)(*i*) $SLL_{ref} = -15$ [dB] by setting the matching threshold to (*a*)(*d*)(*g*) $\eta = 5.0 \times 10^{-2}$ [dB], (*b*)(*e*)(*h*) $\eta = 2.5 \times 10^{-2}$ [dB], and (*c*)(*f*)(*i*) $\eta = 1.25 \times 10^{-2}$ [dB].**

array lattice with $N = 1024$ equi-spaced ($d = \frac{\lambda}{2}$) locations. More specifically, the $K = 7$ elements with indexes $n = \{0, 1, 3, 4, 5, 7, 9\}$ have been turned on [i.e., $b_n = 1$ - black pixel in Fig. 1(*a*)], while the remaining ones have been turned off [i.e., $b_n = 0$ - white pixel in Fig. 1(*a*)]. Figure 1 shows the corresponding samples of the reference array factor, $\mathbf{A}^{ref} = \{\mathcal{A}_m^{ref};\ m = 0, \ldots, N-1\}$, which have been computed through (5) [Fig. 1(*b*)] along with the normalized power pattern values, $\mathbf{P}^{ref} = \{\mathcal{P}_m^{ref}; m = 0, \ldots, N-1\}$ ($\mathcal{P}_m \triangleq |\mathcal{A}_m|^2$) [Fig. 1(*c*)]. The *QC*-thinning method has been then applied to solve the *AATP* where the same array factor function is the pattern 'feature' at hand [i.e., $\mathbb{G}\left\{\mathcal{A}^{ref}(u)\right\} = \mathcal{A}^{ref}(u)$]. Starting from $\mathbf{A}^{ref}$ and applying a cyclic shift such that $m \leftarrow \left(m + \frac{N}{2}\right)\ mod\ N$, the normalized complex amplitudes of the *input quantum state vector* $\left|\mathbf{A}^{ref}\right\rangle$, $\widehat{\mathbf{A}}^{ref}$ ($\widehat{\mathbf{A}}^{ref} = \{\widehat{\mathcal{A}}_m^{ref}; m = 0, \ldots, N-1\}$), have been computed and the *IQFT* has been run, by using $L = 10$ qubits, $R = 2 \times N$ times to statistically validate the arising thinned array solution. Figure 2 gives the values, measured at the output of the *QC* processor simulated within the Qiskit framework, of the probabilities of the output quantum state vector $|\mathbf{w}\rangle$, $\{p_n;\ n = 0, \ldots, N-1\}$. As it can be observed, only the states corresponding to the indexes of the $K = 7$ elements that were active (i.e., $b_n = 1$) in the reference thinned array have a probability p_n different from zero, while the probabilities of all the others $(N - K)$ quantum output states are exactly zero. Moreover, the fact that the probabilities associated to the active elements are equal confirms the effectiveness of the QC-based method in retrieving the isophoric reference arrangement. As for the reliability of the *QC*-based thinning, it is worth pointing out that the same result has been obtained running the *IQFT* for $R = \frac{N}{2}$, $R = N$, and $R = 4 \times N$ times. Of course, a final proof on this matter would be available only running the SW code on a real quantum processor since Qiskit is a realistic

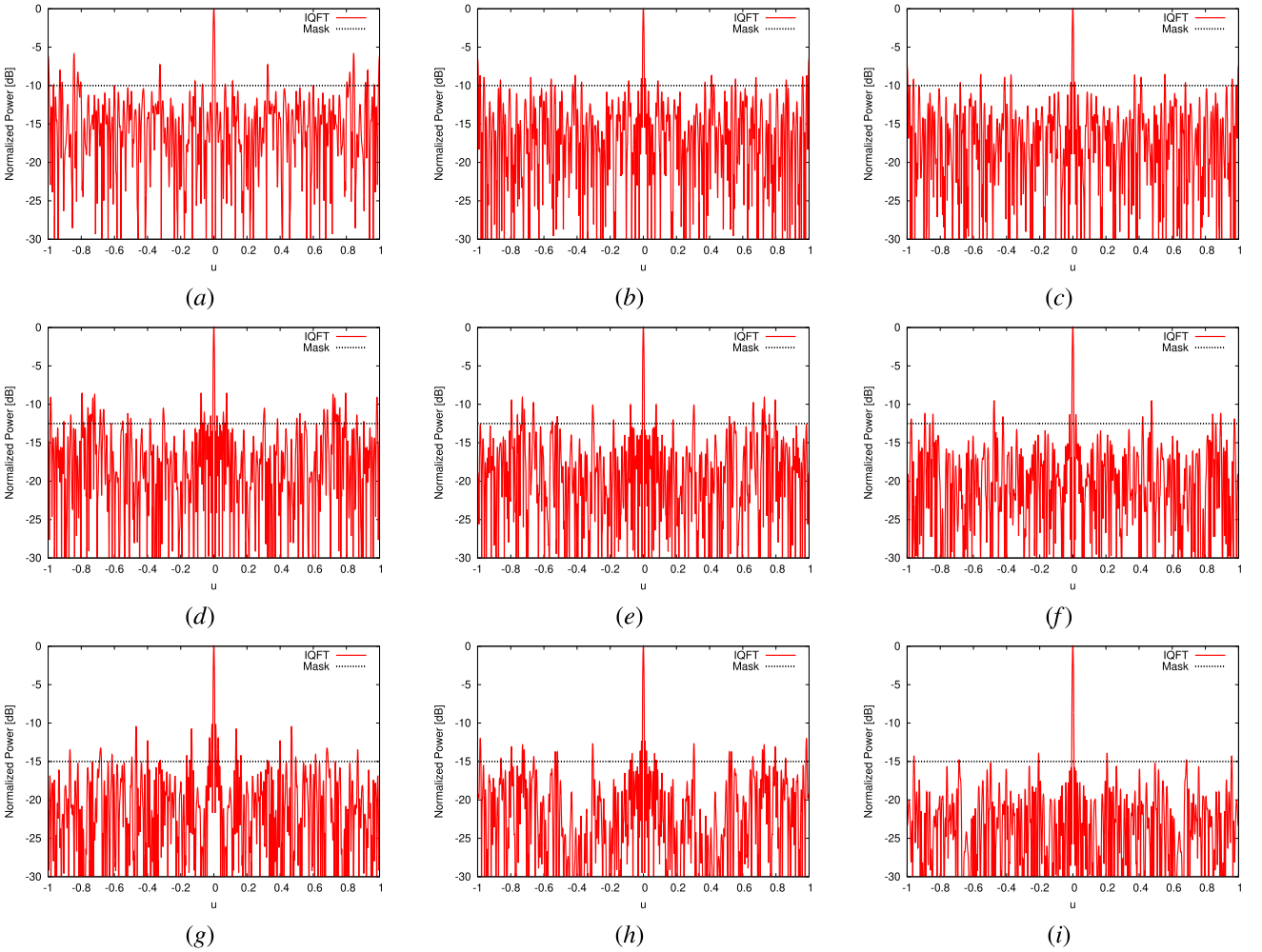

FIGURE 5. ***Numerical Assessment*** **- Plot of the normalized power patterns radiated by the thinned layouts in Fig. 4.**

emulation tool of a *QC* machine. As for the computational issues, the acceleration factor enabled by the *IQFT* with respect to the use of classical *IDFT* to perform the same four-step thinning process is proportional to the ratio $\left(\frac{N}{\log N}\right)$ and, for this example with $N = 1024$, it amounts to 147 times.

The second example (*Analysis*) is devoted to check the robustness of the *QC* thinning to the noise blurring the amplitude of the input quantum vector, $\widehat{\mathbf{A}}^{ref}$. Towards this purpose, the m-th ($m = 0, \ldots, N-1$) noisy amplitude $\widehat{\mathcal{A}}_m^{ref}$ has been computed as follows

$$\widetilde{A}_m^{ref} = \widehat{\mathcal{A}}_m^{ref} + \nu_m \tag{13}$$

where ν_m is the m-th realization of an additive zero-mean complex Gaussian noise with variance σ. By considering different values of the signal-to-noise ratio (*SNR*)

$$SNR \triangleq \frac{\sum_{m=0}^{N-1} \left|\widehat{\mathcal{A}}_m^{ref}\right|^2}{\sum_{m=0}^{N-1} |\nu_m|^2} \tag{14}$$

in the range from 50 [dB] down to 0 [dB] with a step of 10 [dB], each quantum simulation has been repeated $R = 2 \times N$ times. It turns out that the highest probabilities are always associated to the quantum states of the output vector corresponding to the $K = 7$ active elements of the reference thinned array. On the contrary, the probability values of the other $(N - K)$ elements quickly decrease as shown in the sorted list of Fig. 3. More in detail, they reduce of more than one ($SNR = 0$ [dB]), three ($SNR = 10$ [dB]), four ($SNR = 20$ [dB]), five ($SNR = 30$ [dB]), and six ($SNR \geq 40$ [dB]) orders of magnitude (Fig. 3), thus the corresponding antenna elements are kept off (i.e., $b_n = 0$, $n = 0, \ldots, N-1$ and $n \neq \{0, 1, 3, 4, 5, 7, 9\}$) in the final layout of the synthesized thinned array.

In the third example (*Assessment*), the goal of the synthesis is that of thinning a reference lattice of $N = 256$ candidate locations equally-spaced by $d = \frac{\lambda}{2}$ to afford a pattern with a user-defined sidelobe level (*SLL*) (i.e., $\mathbb{G}\left\{\mathcal{A}^{ref}(u)\right\} = SLL_{ref}$) defined as $SLL \triangleq -10 \times \log\left[\max_{u \in \Omega}\left\{\frac{\mathcal{P}^{ref}(0)}{\mathcal{P}^{ref}(u)}\right\}\right]$, Ω and $\mathcal{P}(u)$ being the sidelobe region and the normalized

TABLE 1. ***Numerical Assessment*** **- Descriptive/performance indexes.**

SLL_{ref} [dB]	η $(\times 10^2)$	K	τ [%]	$\overline{SLL}$ [dB]	SLL [dB]	$\aleph$
-10.0	5.0	24	90.62	-14.2	-5.8	20
-10.0	2.5	29	88.67	-14.9	-6.5	18
-10.0	1.25	33	87.11	-15.5	-7.3	12
-12.5	5.0	38	85.16	-16.1	-8.5	38
-12.5	2.5	47	81.64	-17.1	-9.1	20
-12.5	1.25	59	76.95	-18.4	-9.5	12
-15.0	5.0	69	73.05	-19.2	-10.1	24
-15.0	2.5	84	67.19	-20.0	-12.0	22
-15.0	1.25	112	56.25	-21.9	-13.9	6

power pattern ($\mathcal{P}(u) \triangleq |\mathcal{A}(u)|^2$), respectively. Accordingly, $L = 8$ qubits have been used for the *IQFT*, while the non-uniform amplitudes of the array have been set to $\widehat{w}_n = \sqrt{p_n}$ ($n = 0, \ldots, N-1$) (10). A wide set of synthesis tests has been carried out by varying the matching threshold η (i.e., the degree-of-matching with the requirement) for different values of SLL_{ref}. Since in this case the objective is to afford a pattern with a user-defined *SLL*, being $\mathbb{G}\left\{\mathcal{A}^{ref}(u)\right\} = SLL_{ref}$ a requirement on the power pattern enforced by means of a real-valued mask (Fig. 4), random phase values with symmetric distribution have been set for the N input samples of the array factor, $\mathcal{A}_m, m = 0, \ldots, N-1$ (i.e., $\mathcal{A}_m = \mathcal{A}_{N-1-m}$, $m = 0, \ldots, \frac{N}{2} - 1$) to obtain, thanks to the properties of the Fourier transform, the synthesis of real excitations. For illustrative purposes, Figure 4 shows some representative samples of the *QC*-synthesized layouts, while the corresponding patterns are reported in Fig. 5. Moreover, the values of the descriptive/performance indexes for each thinned solution in Fig. 4 are summarized in Tab. 1. As expected, the better the requirement fitting (i.e., a lower value of η), the greater the number of 'on' elements in the reference lattice, K, and the lower the thinning percentage τ ($\tau \triangleq \frac{N-K}{N}$) (Tab. 1). For instance, let us focus on the case of the requirement $SLL_{ref} = -12.5$ [dB]. Decreasing the matching threshold η from $\eta = 5.0 \times 10^{-2}$ down to $\eta = 1.25 \times 10^{-2}$, the number of mask violation $\aleph$ (i.e., the number of u values for which $\mathcal{P}(u)\rfloor_{u\in\Omega} > SLL_{th}$) reduces [i.e., $\aleph]_{\eta=5.0\times10^{-2}}^{SLL_{ref}=-12.5\,[\mathrm{dB}]} = 38$ - Fig. 5(*d*), $\aleph]_{\eta=2.5\times10^{-2}}^{SLL_{ref}=-12.5\,[\mathrm{dB}]} = 20$ - Fig. 5(*e*), and $\aleph]_{\eta=1.25\times10^{-2}}^{SLL_{ref}=-12.5\,[\mathrm{dB}]} = 12$ - Fig. 5(*f*)] as well as the average amplitude of the sidelobes $\overline{SLL}$ ($\overline{SLL} \triangleq \frac{1}{2}\int_{u\in\Omega} \mathcal{P}(u)\,du$) [i.e., $\overline{SLL}]_{\eta=5.0\times10^{-2}}^{SLL_{ref}=-12.5\,[\mathrm{dB}]} = -16.1$ [dB] - Fig. 5(*d*), $\overline{SLL}]_{\eta=2.5\times10^{-2}}^{SLL_{ref}=-12.5\,[\mathrm{dB}]} = -17.1$ [dB] - Fig. 5(*e*), and $\overline{SLL}]_{\eta=1.25\times10^{-2}}^{SLL_{ref}=-12.5\,[\mathrm{dB}]} = -18.4$ [dB] - Fig. 5(*f*)], but the thinning percentage decreases (i.e., $\tau]_{\eta=5.0\times10^{-2}}^{SLL_{ref}=-12.5\,[\mathrm{dB}]} = 85.16\%$, $\tau]_{\eta=2.5\times10^{-2}}^{SLL_{ref}=-12.5\,[\mathrm{dB}]} = 81.64\,\%$, and $\tau]_{\eta=1.25\times10^{-2}}^{SLL_{ref}=-12.5\,[\mathrm{dB}]} = 76.95\,\%$ - Tab. 1) since less elements are turned off [Fig. 4(*d*) vs. Fig. 4(*e*) vs. Fig. 4(*f*)]. On the other hand, keeping fixed the η value, while decreasing the *SLL* threshold SLL_{ref}, implies that more elements need to be activated to maintain almost constant the number of mask violations $\aleph$ (e.g., $\eta = 2.5 \times 10^{-2}$: $K]_{SLL_{ref}=-10\,[\mathrm{dB}]}^{\eta=2.5\times10^{-2}} = 29$ [Fig. 4(*b*)] $\rightarrow$ $\aleph]_{SLL_{ref}=-10\,[\mathrm{dB}]}^{\eta=2.5\times10^{-2}} = 18$, $K]_{SLL_{ref}=-12.5\,[\mathrm{dB}]}^{\eta=2.5\times10^{-2}} = 47$ [Fig. 4(*e*)] $\rightarrow$ $\aleph]_{SLL_{ref}=-12.5\,[\mathrm{dB}]}^{\eta=2.5\times10^{-2}} = 20$, and $K]_{SLL_{ref}=-15\,[\mathrm{dB}]}^{\eta=2.5\times10^{-2}} = 84$ [Fig. 4(*h*)] $\rightarrow$ $\aleph]_{SLL_{ref}=-15\,[\mathrm{dB}]}^{\eta=2.5\times10^{-2}} = 22$). The speed-up of the *QC*-based thinning procedure turns out to be 46 times that of the classical one since $N = 256$ for this example.

Finally, the solutions obtained by means of the proposed *QC*-based approach are compared with the fully-populated arrays synthesized by means of the classical *IDFT*. The synthesized amplitude [Figs. 6(*a*)-(*c*)] and phase [Figs. 6(*d*)-(*f*)] excitation coefficients when considering the same *SLL* target values of Tab. 1, namely $SLL_{ref} = -10.0$ [dB] [Figs. 6(*a*)(*d*)], $SLL_{ref} = -12.5$ [dB] [Figs. 6(*b*)(*e*)], and $SLL_{ref} = -15.0$ [dB] [Figs. 6(*c*)(*f*)] are reported in Fig. 6. Moreover, the corresponding power patterns are shown in Fig. 7 in comparison with the patterns of the thinned arrays synthesized when considering a matching error of $\eta = 1.25 \times 10^{-2}$ for each SLL_{ref} (Tab. 1). As expected, the *IDFT* excitations turns out to be real since the phase coefficients only assume values equal to $\varphi_n = \{-\pi, 0, \pi\}$, $n = 0, \ldots, N-1$ [Figs. 6(*d*)-(*f*)]. However, unlike the *QC*-synthesized excitations, they are characterized by both positive and negative values since $\exp[j\varphi_n]|_{\varphi_n=\pm\pi} = -1$. As for the radiation patterns, the shape of the mainlobes generated from the thinned arrays are very close and in some cases overlap [Figs. 7(*b*)(*c*)] with the ones obtained from the fully-populated solutions. This result is due to the fact that also the *QC*-designed thinned arrays have elements distributed over the whole array aperture (Fig. 4 vs. Fig. 6), being the mainlobe width function of the aperture size (i.e., distance between the first and last active element in the array). As for the sidelobe behavior, the power patterns arising from the *IDFT* more faithfully follow the reference mask, having sidelobes always around (i.e., either above or below) the desired SLL_{ref} value. Differently, the *QC*-thinned arrays allow controlling the *SLL* through the proposed algorithm (Fig. 5 and Tab. 1).

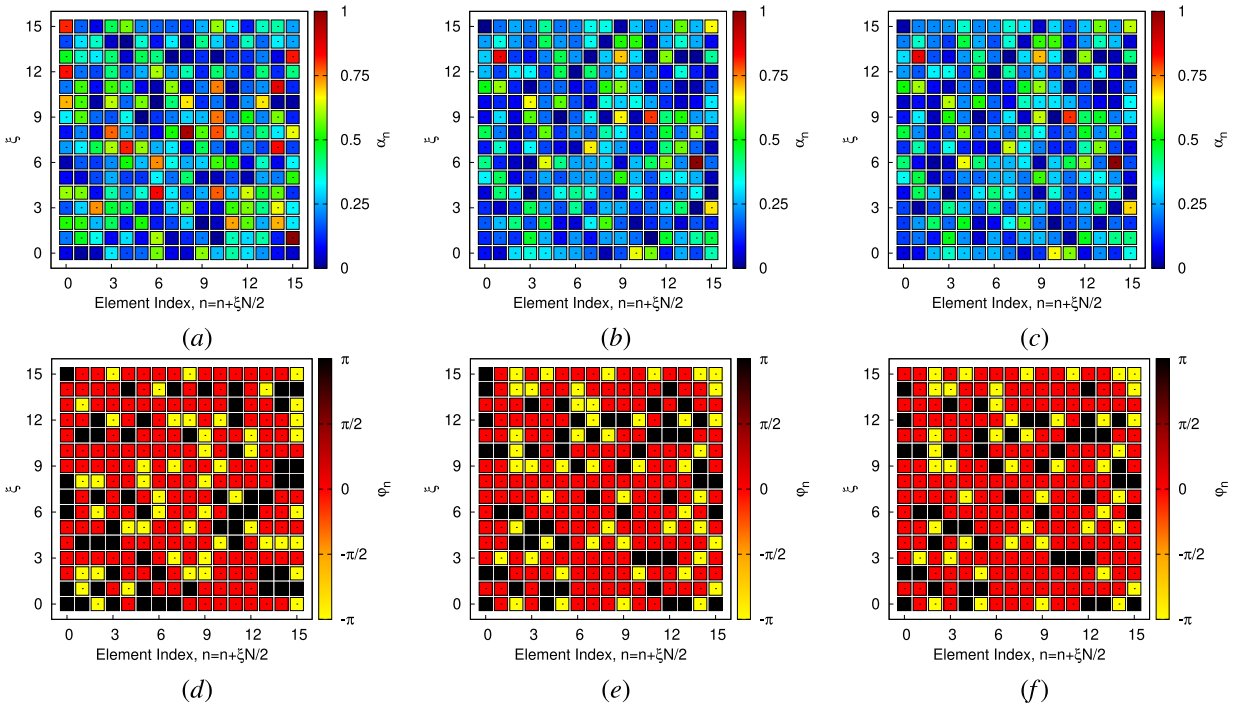

FIGURE 6. *Comparative Assessment - IDFT*-synthesized (*a*)(*b*)(*c*) amplitude and (*d*)(*e*)(*f*) phase excitation coefficients when (*a*)(*d*) $SLL_{ref} = -10.0$ [dB], (*b*)(*e*) $SLL_{ref} = -12.5$ [dB], and (*c*)(*f*) $SLL_{ref} = -15$ [dB].

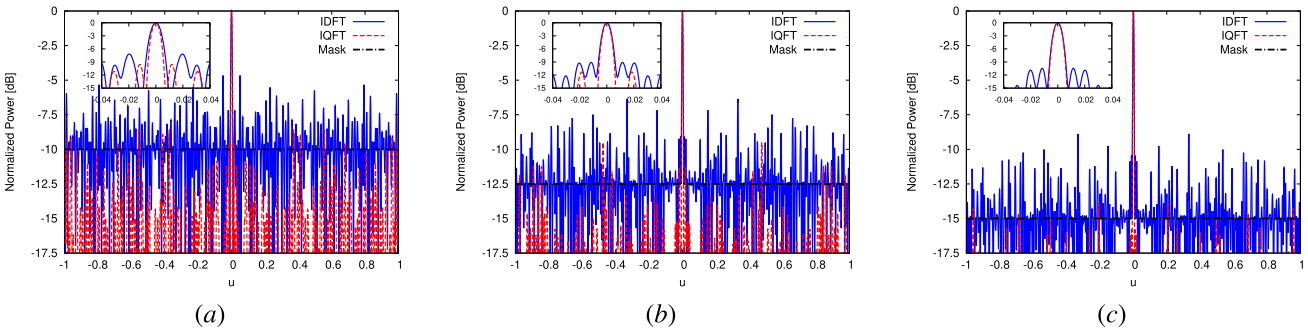

FIGURE 7. *Comparative Assessment* - Plot of the normalized power patterns radiated by the fully-populated arrays in Fig. 6.

IV. CONCLUSION

An innovative procedure based on *QC* has been proposed for the synthesis of thinned antenna arrays. Towards this aim, a strategy based on a customization of the *QFT* algorithm has been developed and a set of representative numerical results has been reported and discussed to give some insights on the features and the potentialities of the proposed approach also in comparison with a classical *DFT* implementation.

To the best of the authors' knowledge, the main innovative contributions of this paper with respect to the state-of-the art lie in the following:

- the formulation of the array thinning problem in the *QC* framework;
- the customization of the *QFT* procedure and the exploitation of the observable probabilities of the output quantum state vector for synthesizing both uniformly (i.e., isophoric) and non-uniformly thinned arrays;
- the exploitation of the quantum mechanics principles of superposition and parallelism to yield an exponential acceleration with respect to the classical *DFT* method, thus doing feasible the efficient (i.e., computationally-admissible) thinning of extremely large arrays once quantum processors with many qubits will be available/ accessible.

Besides the feasibility of a *QC*-based thinning, the numerical results have assessed the reliability and the effectiveness of the proposed *QFT*-based method in thinning antenna arrays.

As a final remark, it is worth pointing out that the use of *QC*-based procedures for antenna array synthesis and analysis is still an unexplored area of research deserving more

studies and investigations. By taking into account that the *DFT* algorithm is at the basis of a wide number of methods for addressing antenna arrays problems [1], [2], it is quite natural that future research activities, beyond the scope of this paper, will be aimed at further leveraging on the peculiarities of *QC* and at exploiting the quantum *supremacy* of its implementations to develop novel breakthrough *QC*-based array methodologies.

ACKNOWLEDGMENT

The author Andrea Massa wishes to thank E. Vico for her never-ending inspiration, support, guidance, and help.

REFERENCES

[1] R. J. Mailloux, *Phased Array Antenna Handbook*, 3rd ed. Boston, MA, USA: Artech House, 2018.

[2] R. L. Haupt, *Antenna Arrays—A Computation Approach*. Hoboken, NJ, USA: Wiley, 2010.

[3] G. Oliveri, G. Gottardi, F. Robol, A. Polo, L. Poli, M. Salucci, M. Chuan, C. Massagrande, P. Vinetti, M. Mattivi, R. Lombardi, and A. Massa, "Codesign of unconventional array architectures and antenna elements for 5G base stations," *IEEE Trans. Antennas Propag.*, vol. 65, no. 12, pp. 6752–6767, Dec. 2017.

[4] C. Mao, M. Khalily, P. Xiao, T. W. C. Brown, and S. Gao, "Planar sub-millimeter-wave array antenna with enhanced gain and reduced sidelobes for 5G broadcast applications," *IEEE Trans. Antennas Propag.*, vol. 67, no. 1, pp. 160–168, Jan. 2019.

[5] J. Zhang, K. Zhao, L. Wang, S. Zhang, and G. F. Pedersen, "Dual-polarized phased array with end-fire radiation for 5G handset applications," *IEEE Trans. Antennas Propag.*, vol. 68, no. 4, pp. 3277–3282, Apr. 2020.

[6] B. Ku, P. Schmalenberg, O. Inac, O. D. Gurbuz, J. S. Lee, K. Shiozaki, and G. M. Rebeiz, "A 77–81-GHz 16-element phased-array receiver with ±50° beam scanning for advanced automotive radars," *IEEE Trans. Microw. Theory Techn.*, vol. 62, no. 11, pp. 2823–2832, Nov. 2014.

[7] M. Harter, J. Hildebrandt, A. Ziroff, and T. Zwick, "Self-calibration of a 3-D-digital beamforming radar system for automotive applications with installation behind automotive covers," *IEEE Trans. Microw. Theory Techn.*, vol. 64, no. 9, pp. 2994–3000, Sep. 2016.

[8] G. F. Hamberger, S. Späth, U. Siart, and T. F. Eibert, "A mixed circular/linear dual-polarized phased array concept for automotive radar—Planar antenna designs and system evaluation at 78 GHz," *IEEE Trans. Antennas Propag.*, vol. 67, no. 3, pp. 1562–1572, Mar. 2019.

[9] J. Herd, S. Duffy, M. Weber, G. Brigham, C. Weigand, and D. Curcio, "Advanced architecture for a low cost multifunction phased array radar," in *IEEE MTT-S Int. Microw. Symp. Dig.*, Anaheim, CA, USA, May 2010, pp. 676–679.

[10] J. E. Stailey and K. D. Hondl, "Multifunction phased array radar for aircraft and weather surveillance," *Proc. IEEE*, vol. 104, no. 3, pp. 649–659, Mar. 2016.

[11] J. D. Díaz, J. L. Salazar-Cerreno, J. A. Ortiz, N. A. Aboserwal, R. M. Lebrón, C. Fulton, and R. D. Palmer, "A cross-stacked radiating antenna with enhanced scanning performance for digital beamforming multifunction phased-array radars," *IEEE Trans. Antennas Propag.*, vol. 66, no. 10, pp. 5258–5267, Oct. 2018.

[12] O. M. Bucci, L. Crocco, R. Scapaticci, and G. Bellizzi, "On the design of phased arrays for medical applications," *Proc. IEEE*, vol. 104, no. 3, pp. 633–648, Mar. 2016.

[13] D. B. Rodrigues, J. Ellsworth, and P. Turner, "Feasibility of heating brain tumors using a 915 MHz annular phased-array," *IEEE Antennas Wireless Propag. Lett.*, vol. 20, no. 4, pp. 423–427, Apr. 2021.

[14] P. Rocca, G. Oliveri, R. J. Mailloux, and A. Massa, "Unconventional phased array architectures and design methodologies—A review," *Proc. IEEE*, vol. 104, no. 3, pp. 544–560, Mar. 2016.

[15] J. S. Herd and M. D. Conway, "The evolution to modern phased array architectures," *Proc. IEEE*, vol. 104, no. 3, pp. 519–529, Mar. 2016.

[16] P. Lopez, J. A. Rodriguez, F. Ares, and E. Moreno, "Subarray weighting for difference patterns of monopulse antennas: Joint optimization of subarray configurations and weights," *IEEE Trans. Antennas Propag.*, vol. 49, no. 11, pp. 1606–1608, Nov. 2001.

[17] R. L. Haupt, "Optimized weighting of uniform subarrays of unequal sizes," *IEEE Trans. Antennas Propag.*, vol. 55, no. 4, pp. 1207–1210, Apr. 2007.

[18] P. Rocca, L. Manica, and A. Massa, "An improved excitation matching method based on an ant colony optimization for suboptimal-free clustering in sum-difference compromise synthesis," *IEEE Trans. Antennas Propag.*, vol. 57, no. 8, pp. 2297–2306, Aug. 2009.

[19] L. Manica, P. Rocca, G. Oliveri, and A. Massa, "Synthesis of multi-beam sub-arrayed antennas through an excitation matching strategy," *IEEE Trans. Antennas Propag.*, vol. 59, no. 2, pp. 482–492, Feb. 2011.

[20] N. Anselmi, P. Rocca, M. Salucci, and A. Massa, "Contiguous phase-clustering in multibeam-on-receive scanning arrays," *IEEE Trans. Antennas Propag.*, vol. 66, no. 11, pp. 5879–5891, Nov. 2018.

[21] G. Oliveri and A. Massa, "Bayesian compressive sampling for pattern synthesis with maximally sparse non-uniform linear arrays," *IEEE Trans. Antennas Propag.*, vol. 59, no. 2, pp. 467–481, Feb. 2011.

[22] F. Viani, G. Oliveri, and A. Massa, "Compressive sensing pattern matching techniques for synthesizing planar sparse arrays," *IEEE Trans. Antennas Propag.*, vol. 61, no. 9, pp. 4577–4587, Sep. 2013.

[23] O. M. Bucci, T. Isernia, S. Perna, and D. Pinchera, "Isophoric sparse arrays ensuring global coverage in satellite communications," *IEEE Trans. Antennas Propag.*, vol. 62, no. 4, pp. 1607–1618, Apr. 2014.

[24] A. F. Morabito, A. Di Carlo, L. Di Donato, T. Isernia, and G. Sorbello, "Extending spectral factorization to array pattern synthesis including sparseness, mutual coupling, and mounting-platform effects," *IEEE Trans. Antennas Propag.*, vol. 67, no. 7, pp. 4548–4559, Jul. 2019.

[25] M. I. Skolnik, J. Sherman, III, and F. Ogg, Jr., "Statistically designed density-tapered arrays," *IEEE Trans. Antennas Propag.*, vol. AP-12, no. 4, pp. 408–417, Jul. 1964.

[26] Y. T. Lo, "A mathematical theory of antenna arrays with randomly spaced elements," *IEEE Trans. Antennas Propag.*, vol. AP-12, no. 3, pp. 257–268, May 1964.

[27] A. T. V. Murino and C. S. Regazzoni, "Synthesis of unequally spaced arrays by simulated annealing," *IEEE Trans. Signal Process.*, vol. 44, no. 1, pp. 119–123, Jan. 1996.

[28] R. L. Haupt, "Thinned arrays using genetic algorithms," *IEEE Trans. Antennas Propag.*, vol. 42, no. 7, pp. 993–999, Jul. 1994.

[29] G. Oliveri, M. Donelli, and A. Massa, "Genetically-designed arbitrary length almost difference sets," *Electron. Lett.*, vol. 5, no. 23, pp. 1182–1183, Nov. 2009.

[30] M. Donelli, A. Martini, and A. Massa, "A hybrid approach based on PSO and Hadamard difference sets for the synthesis of square thinned arrays," *IEEE Trans. Antennas Propag.*, vol. 57, no. 8, pp. 2491–2495, Aug. 2009.

[31] O. Quevedo-Teruel and E. Rajo-Iglesias, "Ant colony optimization in thinned array synthesis with minimum sidelobe level," *IEEE Antennas Wireless Propag. Lett.*, vol. 5, pp. 349–352, 2006.

[32] G. Oliveri, M. Donelli, and A. Massa, "Linear array thinning exploiting almost difference sets," *IEEE Trans. Antennas Propag.*, vol. 57, no. 12, pp. 3800–3812, Dec. 2009.

[33] G. Oliveri, G. Gottardi, M. A. Hannan, N. Anselmi, and L. Poli, "Autocorrelation-driven synthesis of antenna arrays—The case of DS-based planar isophoric thinned arrays," *IEEE Trans. Antennas Propag.*, vol. 68, no. 4, pp. 2895–2910, Apr. 2020.

[34] D. Sartori, G. Oliveri, L. Manica, and A. Massa, "Hybrid design of non-regular linear arrays with accurate control of the pattern sidelobes," *IEEE Trans. Antennas Propag.*, vol. 61, no. 12, pp. 6237–6242, Dec. 2013.

[35] N. Anselmi, L. Poli, P. Rocca, and A. Massa, "Design of simplified array layouts for preliminary experimental testing and validation of large AESAs," *IEEE Trans. Antennas Propag.*, vol. 66, no. 12, pp. 6906–6920, Dec. 2018.

[36] M. Nielsen and I. Chuang, *Quantum Computation and Quantum Information*. Cambridge, MA, USA: Cambridge Univ. Press, 2000.

[37] P. W. Shor, "Polynomial-time algorithms for prime factorization and discrete logarithms on a quantum computer," *SIAM Rev.*, vol. 41, no. 2, pp. 303–332, Jan. 1999.

[38] M. M. Wilde, *Quantum Information Theory*, 2nd ed. Cambridge, U.K.: Cambridge Univ. Press, 2017.

[39] G. Aleksandrowicz *et al.*, "Qiskit: An open-source framework for quantum computing (0.7.2)," Zenodo, Eur. Org. Nucl. Res., CERN, Jan. 2019. Accessed: May 13, 2021, doi: 10.5281/zenodo.2562110.

[40] *IBM Quantum*. Accessed: May 31, 2021. [Online]. Available: https://quantum-computing.ibm.com

PAOLO ROCCA (Senior Member, IEEE) received the M.S. degree *(summa cum laude)* in telecommunications engineering and the Ph.D. degree in information and communication technologies from the University of Trento, Italy, in 2005 and 2008, respectively.

He is currently an Associate Professor with the Department of Information Engineering and Computer Science, University of Trento, the Huashan Scholar Chair Professor with Xidian University, Xi'an, China, and a member of the ELEDIA Research Center. He received the National Scientific Qualification for the position of a Full Professor in Italy and France, in April 2017 and January 2020, respectively. He has been a Visiting Ph.D. Student with Pennsylvania State University, USA, and the University Mediterranea of Reggio Calabria, Italy, and a Visiting Researcher with the Laboratoire des Signaux et Systèmes (L2S), Supèlec, France, in 2012 and 2013. Moreover, he has been an Invited Professor with the University of Paris Sud, France, in 2015, and the University of Rennes 1, France, in 2017. He is the author or coauthor of one book chapter, 140 journals, and more than 270 conference papers. His research interests include the framework of artificial intelligence techniques as applied to electromagnetics, antenna array synthesis and analysis, and electromagnetic inverse scattering. He has been awarded from the IEEE Geoscience and Remote Sensing Society and the Italy Section with the Best Ph.D. Thesis Award IEEE-GRS Central Italy Chapter. He served as an Associate Editor for the IEEE Antennas and Wireless Propagation Letters (2011–2016) and the *Microwave and Optical Technology Letters* (2019–2020). He has been serving as an Associate Editor for the *IEEE Antennas and Propagation Magazine*, since 2020, and *Engineering*, since 2020. He was the Guest Editor of the IEEE Antennas and Wireless Propagation Letters for the 2020 Special Cluster on "Space-Time Modulated Antennas and Materials."

NICOLA ANSELMI (Member, IEEE) received the M.S. degree in telecommunication engineering from the University of Trento, Italy, in 2012, and the Ph.D. degree from the International Doctoral School, Information and Communication Technology, Trento, Italy, in 2018.

He is currently an Assistant Professor with the Department of Information Engineering and Computer Science (DISI), University of Trento, and a Research Fellow of the ELEDIA Research Center. His research interests include synthesis methods for unconventional antenna array architectures, tolerance analysis of antenna systems, and electromagnetic inverse scattering techniques, with interest on compressive sensing methodologies for microwave imaging applications.

Dr. Anselmi is a member of the IEEE Antennas and Propagation Society. He is also serving as a Reviewer for different international journals, including IEEE Transactions on Antennas and Propagation, IEEE Antennas and Wireless Propagation Letters, and *IET on Microwaves, Antennas & Propagation*. In 2019, he received the Italian National Scientific Qualification for the position of an Associate Professor and the Qualification aux fonctions de maître de conférences. He was a recipient of the "Giorgio Barzilai" Award for the Young Researchers by the Italian Electromagnetic Society (SIEM), in 2016, the "Young Scientis" Prize by the Applied Computational Electromagnetics Society (ACES), in 2018, and the "Mini-Circuits Harvey Kaylie Best Paper Prize" by the IEEE International Conference on Microwaves, Communications, Antennas & Electronic Systems (COMCAS), in 2019.

GIACOMO OLIVERI (Senior Member, IEEE) received the B.S. and M.S. degrees in telecommunications engineering and the Ph.D. degree in space sciences and engineering from the University of Genoa, Italy, in 2003, 2005, and 2009, respectively.

He is currently an Associate Professor with the Department of Information Engineering and Computer Science, University of Trento, and a Board Member of the ELEDIA Research Center. He is also an Adjunct Professor with CentraleSupélec and a member of the Laboratoire des Signaux et Systémes (L2S), CentraleSupélec Gif-sur-Yvette, France. He has been a Visiting Researcher at L2S, in 2012, 2013, and 2015, an Invited Associate Professor, in 2014, and a Visiting Professor with Université Paris-Saclay, France, in 2016 and 2017. He is the author or coauthor of over 400 peer-reviewed articles on international journals and conferences. His research interests include electromagnetic direct and inverse problems, system-by-design and metamaterials, and antenna array synthesis. He is the Chair of the IEEE AP/ED/MTT North Italy Chapter. He serves as an Associate Editor for the IEEE Antennas and Wireless Propagation Letters, the IEEE Journal on Multiscale and Multiphysics Computational Techniques, the *International Journal of Antennas and Propagation*, the *International Journal of Distributed Sensor Networks*, the *Microwave Processing* journal, and the *Sensors* journal.

ALESSANDRO POLO (Member, IEEE) received the M.S. degree in telecommunication engineering from the University of Trento, Italy, in 2012, and the Ph.D. degree from the International Doctoral School, Information and Communication Technology of Trento, in 2018.

From 2018 to 2019, he was a Visiting Postdoctoral Researcher with the Radiocommunications Laboratory, Department of Physics, Aristotle University of Thessaloniki, Thessaloniki, Greece. He received the National Scientific Qualification for the position of an Associate Professor, Italy, in November 2020. He is currently a Postdoctoral Researcher with the Department of Information Engineering and Computer Science (DISI), University of Trento, and a Research Fellow of the ELEDIA Research Center. His research interests include wireless localization and networking, antenna systems, distributed computing, decision support systems for fleet, and emergency/critical applications. He has a long experience in the fields of KPI analysis and troubleshooting, machine learning, and optimization techniques.

Prof. Polo was a recipient of the "Yarman-Carlin Student Paper" Award at the IEEE Mediterranean Microwave Symposium, in 2015, and the InSIEm Award for the paper "Decision suppOrt system for fleet Management and mIssioN cOntrol—DOMiNO" presented at the XX Riunione Nazionale di Elettromagnetismo in Padua, Italy, in 2014. He serves as an Associate Editor for the journal of *Telecom*, *Journal of Engineering*, and *Journal of Networking and Telecommunications*.

ANDREA MASSA (Fellow, IEEE) received the Laurea (M.S.) degree in electronic engineering and the Ph.D. degree in EECS from the University of Genoa, Genoa, Italy, in 1992 and 1996, respectively.

He is currently a Full Professor of electromagnetic fields with the University of Trento, where he also teaches electromagnetic fields, inverse scattering techniques, antennas and wireless communications, wireless services and devices,

and optimization techniques. He is the Director of Network of Federated Laboratories ''ELEDIA Research Center'' (www.eledia.org) located in Brunei, China, Czech, France, Greece, Italy, Japan, Peru, and Tunisia with more than 150 researchers. He is also the holder of Chang-Jiang Chair Professorship at UESTC, Chengdu, China, a Professor at CentraleSupélec, Paris, France, and a Visiting Professor at Tsinghua, Beijing, China. He has been the holder of Senior DIGITEO Chair at L2S, CentraleSupélec, and CEA LIST in Saclay, France, the UC3M-Santander Chair of Excellence with the Universidad Carlos III de Madrid, Spain, an Adjunct Professor at Penn State University, USA, a Guest Professor at UESTC, China, and a Visiting Professor at Missouri University of Science and Technology, USA, Nagasaki University, Japan, the University of Paris Sud, France, Kumamoto University, Japan, and the National University of Singapore, Singapore. He has published more than 700 scientific publications among which more than 350 on international journals (more than 12.000 citations—H-index is 55 [Scopus]; more than 9.500 citations—H-index is 48 [ISI-WoS]; more than 20.000 citations—H-index is 80 [Google Scholar]) and more than 500 in international conferences where he presented more than 200 invited contributions (more than 35 invited keynote speaker) (www.eledia.org/publications). He has organized more than 100 scientific sessions in international conferences and has participated to several technological projects in the European framework (more than 20 EU Projects) as well as at the national and local level with national agencies (more than 300 Projects/Grants). His research interests include inverse problems, analysis/synthesis of antenna systems and large arrays, radar systems synthesis and signal processing, cross layer optimization and planning of wireless/RF systems, semantic wireless technologies, system-by-design and material by design (metamaterials and reconfigurable materials), and theory/applications of optimization techniques to engineering problems (telecommunications, medicine, and biology). He is a fellow of IET and the Electromagnetic Academy.

Prof. Massa has been appointed as a IEEE AP-S Distinguished Lecturer (2016–2018) and served as an Associate Editor for the IEEE TRANSACTION ON ANTENNAS AND PROPAGATION (2011–2014). He serves as an Associate Editor for the *International Journal of Microwave and Wireless Technologies*. He is a member of the Editorial Board of the *Journal of Electromagnetic Waves and Applications*, a Permanent Member of the ''PIERS Technical Committee'' and the ''EuMW Technical Committee,'' and a ESoA Member. He has been appointed in the Scientific Board of the Società Italiana di Elettromagnetismo (SIEm) and elected in the Scientific Board of the Interuniversity National Center for Telecommunications (CNIT). He has been appointed in 2011 by the National Agency for the Evaluation of the University System and National Research (ANVUR) as a member of the Recognized Expert Evaluation Group (Area 09, ''Industrial and Information Engineering'') for the evaluation of the researches at the Italian University and Research Center for the period (2004–2010). Furthermore, he has been elected as an Italian Member of the Management Committee of the COST Action TU1208 ''Civil Engineering Applications of Ground Penetrating Radar.''